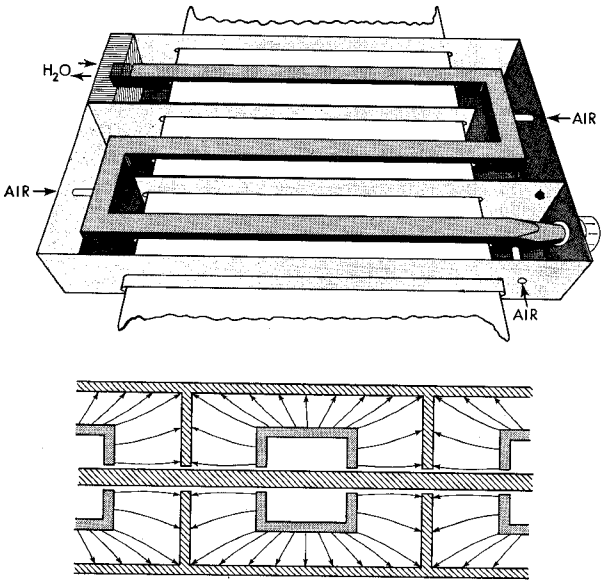

Fig. 5. Schematic diagram of a complete applicator.

uneven and the temperature quite high, thermal runaway and scorching can result. As the fields near the web are reduced to control attenuation, leakage from the slots will also be reduced. Experiments with a Narda 8110 Radiation Monitor [9] showed that leakage power is proportional to attenuation and otherwise unchanged by going from TE_{10} rectangular waveguide to a TEM structure with the same wall thickness and web load. All these problems are compounded by thick or very wet webs and the TEM structure thus permits heating heavier loads.

Fig. 5 shows a sketch of an implementation of this system. Air can be introduced through chokes or dielectric ducts, flowing from the center conductor directly over the web. The inner conductor can be formed from channel aluminum, rounded at the corners to prevent arcing. The front face, or the dividers, can be set at an angle to control uneven heating. If the center conductor is fairly wide, the spacing to the upper and lower ground plane will dominate the characteristic impedance, permitting reduced sensitivity to manufacturing irregularities.

Conclusions

It has been shown that by going to the TEM mode it is possible to build a simple web applicator that is well designed for both microwave power and air. The applicator size can be reduced for 915 MHz and there is, in principle, no lower frequency limit. Perturbation theory has been found to handle the analysis adequately as is expected for light dielectric loads. Better methods are available to control electric fields in the vicinity of the web and thus the structure is adaptable to a much wider variety of loads.

References

[1] D. A. Dunn, "Slow wave couplers for microwave dielectric heating systems," *J. Microwave Power*, vol. 2, p. 7, 1967.
[2] J. R. White, "Sealing of plastics," in *Microwave Power Engineering*, vol. 2, E. C. Okress, Ed. New York: Academic Press, 1968, p. 122.
[3] P. Jurgensen, "Fringing field applicators," presented at IMPI Symp. (Monterey, Calif., May 25, 1971), Paper 8.2.
[4] J. L. Altman, *Microwave Circuits*. New York: Van Nostrand, 1964.
[5] W. A. G. Voss and W. R. Tinga, "Materials evaluation and measurement techniques," in *Microwave Power Engineering*, vol. 2, E. C. Okress, Ed. New York: Academic Press, 1968, p. 192.
[6] E. V. Jull, W. J. Bleackley, and M. M. Steen, "The design of waveguides with symmetrically placed double ridges," *IEEE Trans. Microwave Theory Tech.* (Corresp.), vol. MTT-17, pp. 397–399, July 1969.
[7] N. H. Williams, "Moisture levelling in paper, wood, textiles and other mixed dielectric sheets," *J. Microwave Power*, vol. 1, pp. 73–80, 1966.
[8] W. R. Tinga, "Dielectric properties of Douglas fir at 2.45 GHz," *J. Microwave Power*, vol. 4, pp. 162–164, Oct. 1969.
[9] E. E. Aslan, "Electromagnetic radiation meter," *IEEE Trans. Microwave Theory Tech. (Special Issue on Biological Effects of Microwaves)* (Corresp.), vol. MTT-19, pp. 249–250, Feb. 1971.

Feedthrough for Digital Latching Ferrite Phasers

J. D. HANFLING AND S. R. MONAGHAN

***Abstract*—Feedthroughs are used in latching ferrite phasers having control wires entering the microwave region. The feedthrough damps out the troublesome resonances that occur as a result of air gaps at the ferrite–waveguide wall interface and at the same time chokes out the radiation from the holes through which the latching wires pass. The equations and curves necessary to design the feedthrough are presented, as well as some experimental results obtained at *C* band on a practical production configuration.**

Introduction

In digital latching ferrite phasers, the presence of air gaps between the surface of the ferrite and the walls of the waveguide cause higher order modes to be excited which couple onto the latching wires and can cause absorption resonances in the dominant-mode output and excessive radiation leakage out of the waveguide. The amount of higher order mode excitation, and consequently the coupling, depends upon the size of the air gap; small air gaps of the order of 0.0003 wavelength can cause relatively large coupling. Although special techniques have been applied to reduce these air gaps, such as finish grinding the ferrite surface flat and using some sort of prestressed cover for the waveguide, air gaps that can significantly degrade performance still occur. Instead of going to extremes with these expensive and time-consuming measures to prevent the air gaps from occurring, the effects of the higher mode excitation can be eliminated cheaply and efficiently by terminating the latching wires in a feedthrough that damps out the resonances and chokes out the radiation leakage.

In the past, tubes of lossy dielectric were placed on the wires or in the waveguide walls through which the wires pass. These tubes produced some damping of resonances, but exhibited high RF leakage and increased the overall loss of the device. Recently, resonances have been damped by a resistive sheet across the guide [1]. The concept of this feedthrough is to introduce a very low impedance at the wire exit hole, giving low RF leakage (good isolation), and to effect a damping of resonances by adding loss outside the propagating waveguide. Design equations and curves are presented for choosing both the dimensions of the device and the type of material. Also described are a theory of operation of the feedthrough and experimental results at *C* band obtained using different types of lossy dielectric as the feedthrough material in a production design.

Theory of Feedthrough Operation

The dimensions of the feedthrough are shown in Fig. 1. The shank of the feedthrough fits into a hole in the side of the waveguide and the latching wire is brought out through the center of the feedthrough and is soldered to the hat. The outer diameter is chosen such that a very low impedance appears at the wire exit hole. The outside wall of the waveguide acts as one conductor of the radial line while the hat of the feedthrough acts as the other. The feedthrough should be made as thin as possible so that the characteristic impedance of the radial line at $r=a$ is small, making the normalized impedance very high at that point. The size of the mismatch as transformed to the input of the radial line determines the isolation achieved. The characteristic impedance of the radial line at $r=a$ is given by

$$Z_0(a) = \frac{b}{2\pi a}\sqrt{\frac{\mu}{\epsilon}} \tag{1}$$

where

μ permeability of radial line material,
ϵ permittivity of radial line material,

Manuscript received August 2, 1971; revised February 15, 1972.
The authors are with the Missile Systems Division, Raytheon Company, Bedford, Mass. 01730.

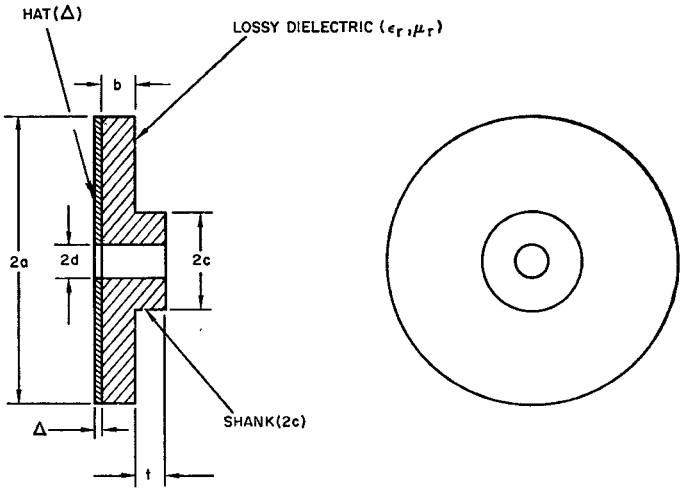

2a = SMALLER THAN THE HEIGHT OF THE WAVEGUIDE
b = 0.010 (OR AS SMALL AS POSSIBLE)
2c = (AS SMALL AS POSSIBLE)
2d = LARGE ENOUGH TO PASS LATCHING WIRE
Δ = AT LEAST FIVE TIMES SKIN DEPTH OF METAL
t = WALL THICKNESS OF WAVEGUIDE

Fig. 1. Feedthrough for digital latching ferrite phasers.

b thickness of radial line,
a outside diameter of radial line.

The normalized impedance at the input to the radial line is given by [2]

$$\frac{Z(c)}{Z_0(c)} = \frac{Z(a)C_t(x,y) + jZ_0(a)\zeta(x,y)}{Z_0(a)\zeta(x,y)c_t(x,y) + jZ(a)} \tag{2}$$

where $x = 2\pi c/\lambda$, $y = 2\pi a/\lambda$, in which λ is the wavelength in the radial line, and $Z(a) = \sqrt{\mu_0/\epsilon_0}$ is the characteristic impedance of free space which terminates the radial line. $C_t(x, y)$, $c_t(x, y)$, and $\zeta(x, y)$ are combinations of first- and second-order Bessel functions.

The radial line is designed so that $Z_0(a) \ll Z(a)$. Therefore,

$$\frac{Z(c)}{Z_0(c)} \approx \zeta(x,y)\frac{Z_0(a)}{Z(a)} - jC_t(x,y) \tag{3}$$

where

$$C_t(x,y) = \frac{J_1(y)N_0(x) - N_1(y)J_0(x)}{J_1(x)N_1(y) - J_1(y)N_1(x)} \tag{4}$$

$$\zeta(x,y) = \frac{J_0(x)N_0(y) - N_0(x)J_0(y)}{J_1(x)N_1(y) - N_1(x)J_1(y)}. \tag{5}$$

By choosing dimensions such that $C_t(x, y) \approx 0$, then

$$\frac{N_0(x)}{J_0(x)} = \frac{N_1(y)}{J_1(y)}. \tag{6}$$

The curves in Fig. 2 give values of x and y for which $C_t(x, y) = 0$; for example,

$$\frac{N_0(1.2)}{J_0(1.2)} = \frac{N_1(2.5)}{J_1(2.5)} = 0.3. \tag{7}$$

This results in a simple expression for the input impedance and VSWR S of the line

$$Z'(c) = \frac{Z(c)}{Z_0(c)} = \zeta(x,y)\frac{Z_0(a)}{Z(a)} \tag{8}$$

$$S = \frac{1}{Z'(c)} = \frac{2\pi a}{b}\sqrt{\frac{\epsilon_r}{\mu_r}}\frac{1}{\zeta(x,y)} \tag{9}$$

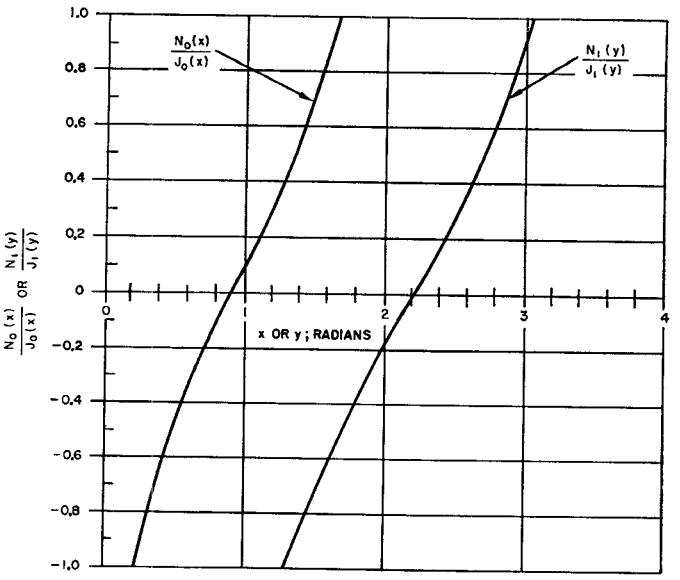

Fig. 2. Conditions for $C_t(x, y) = 0$.

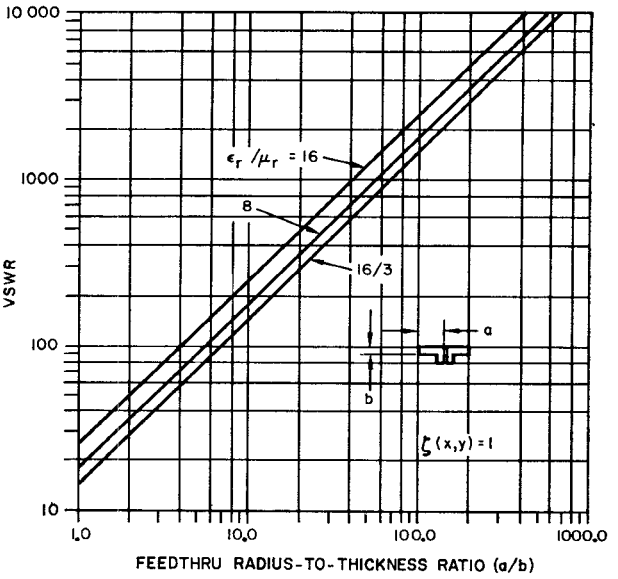

Fig. 3. VSWR versus radius-to-thickness ratio of radial line.

where ϵ_r = permittivity of radial line relative to free space and μ_r = permeability of radial line relative to free space.

Fig. 3 is a plot of (9) for $\zeta(x, y) = 1$ and for three different values of the parameter ϵ_r/μ_r. The values of these parameters were chosen to represent commercially available materials that might possibly be used; for example, $\epsilon_r/\mu_r = 16/3$ corresponds to Emerson Cummings MF 116, an iron-loaded plastic material.

An approximate estimate of the isolation I provided by the feedthrough is

$$I = 20 \log \frac{2\sqrt{S}}{S+1} + 20 \log n \tag{10}$$

where the mode coupling n indicates how much energy is coupled out of the dominant waveguide mode onto the wire. Depending upon the amount of isolation desired, (10) can be used in conjunction with Figs. 2 and 3 for choosing feedthrough dimensions.

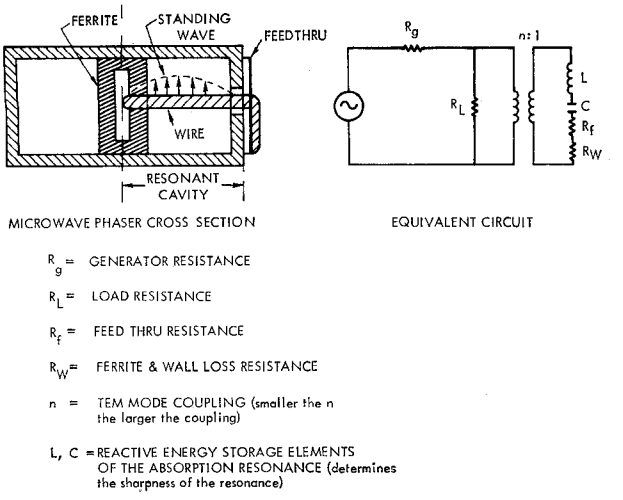

Fig. 4. Dominant-mode equivalent circuit for TEM absorption resonance.

The excitation of higher order modes in the ferrite-loaded waveguide can cause a TEM standing-wave resonance to exist on the latching wire. However, by choosing the loss tangent of the feedthrough material as large as possible while still maintaining the impedance transforming action for isolation, the resulting resonance will be damped out. It should be noted that the maximum loss tangent that can be used is limited by the allowable video circuit resistance between the waveguide wall and the metalized hat of the feedthrough. The RF equivalent circuit of the TEM mode absorption resonance is shown in Fig. 4.

The feedthrough is selected to be the predominant lossy element of the resonant circuit. Neglecting ferrite and wall losses and setting $R_g = R_L$, the absorption at resonance is given in terms of loss tangent and mode coupling by

$$\alpha = \frac{1 + 2n^2 \tan \delta}{2n^2 \tan \delta} \tag{11}$$

where α is the ratio of signal output when there is no resonance to that at the resonant dip. This is derived from the lumped equivalent circuit of Fig. 4 where $\tan \delta = R_f/R_g$. The amount of TEM mode coupling n depends on the reltaive propagation constants of the dominant and spurious modes and on the size of the air gaps between the ferrite and the waveguide wall. In the latching phaser, the coupling parameter is also a function of the bit state, which when reversed can cause a 10- to 14-percent change in the dominant-mode guide wavelength. Fig. 5 is a plot of (11) for mode-coupling values between 5 dB and 40 dB down from incident.

Feedthrough Design

For the digital latching phaser of the cross section shown in Fig. 6 [3], experiments have shown that when no feedthroughs are present, the average amount of energy coupled out onto the wires is about 23 dB down. The total isolation achievable with a feedthrough is limited by the height of the waveguide and how fragile the device can be. For these reasons the outer diameter of the feedthrough is constrained by the 0.3-in height of the waveguide; the thickness of the hat b should be not less than 0.010 in and the diameter of the shank $2c$ not less than 0.100 in. Also, the hole in the shank must be able to pass a no. 28 (0.013) wire. Using these ground rules, the following feedthrough was designed. Assuming λ_0 (free-space wavelength) = 2.5 in, $c = 0.050$ in, $b = 0.010$ in, $\mu_r = 3$, and $\epsilon_r = 16$, then

$$x = \frac{2\pi c}{\lambda_0}\sqrt{\mu_r \epsilon_r} = 0.87$$

and from (6) and the curve of Fig. 2

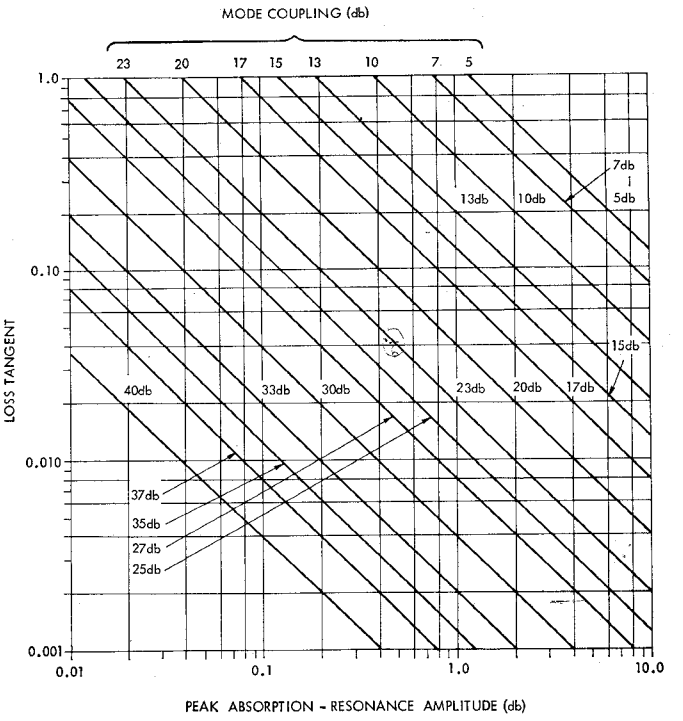

Fig. 5. Loss tangent versus peak absorption-resonance amplitude for several mode-coupling values.

$$\frac{N_0(x)}{J_0(x)} = \frac{N_1(y)}{J_1(y)} \approx 0$$

$$y = \frac{2\pi a}{\lambda}\sqrt{\mu_r \epsilon_r} = 2.2.$$

Therefore, $a = 0.127$ in and $a/b = 12.7$.

The performance of a feedthrough using MF 116 is as follows: From $a/b = 12.7$, the corresponding VSWR from Fig. 3 is 180 and the corresponding isolation is 17 dB; adding 23 dB for average mode coupling and 2 dB for the transmission loss through the feedthrough results in a total isolation of 42 dB. Assuming that the effective loss tangent (electric = 0.08, magnetic = 0.12) is approximately 0.15 and using Fig. 5, the amplitude dip at resonance is 0.085 dB. Feedthroughs of this approximate design and performance, shown in Fig. 6, are presently being produced with copper molded in place for about 15 cents each.

Experimental Results

Several experiments were conducted to demonstrate typical performance capabilities of the feedthrough. In the first experiment, ten digital latching ferrite phase shifters of the cross section of Fig. 6 were constructed maintaining the maximum air gap to less than 0.0003 wavelength and using feedthroughs of the type discussed, but with a loss tangent of 0.01. Swept frequency measurements of insertion loss were made on all units and the average value of the peak resonance was found to be 2.0 dB. Using these results and Fig. 5, the average mode-coupling value is computed to be 23 dB, with variations between 17 and 30 dB.

To improve this performance, tighter tolerance control during fabrication is required or a lossier feedthrough must be used. If we assume that the amount of coupling is directly proportional to the size of the air gaps present, then in order to achieve 0.1 to 0.2 dB average peak absorption amplitude at resonance, the mode coupling would have to be reduced to the 33 to 35 level. This corresponds to a 3 to 4:1 reduction in air gaps or the use of a feedthrough material having a loss tangent between 0.1 and 0.2.

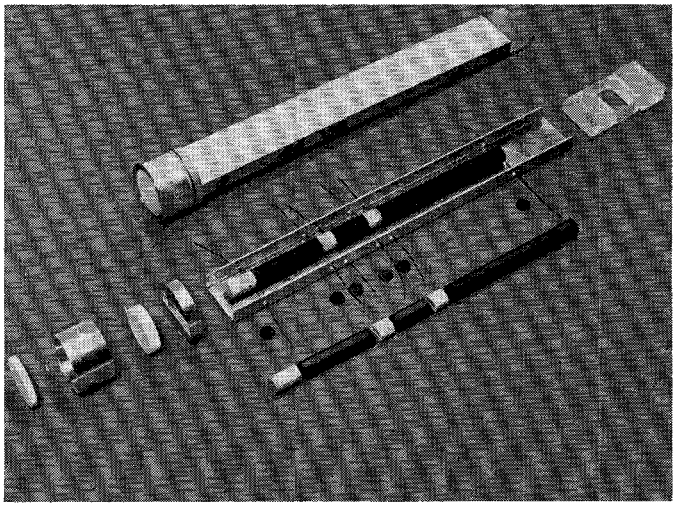

Fig. 6. Developmental array phaser showing feedthroughs.

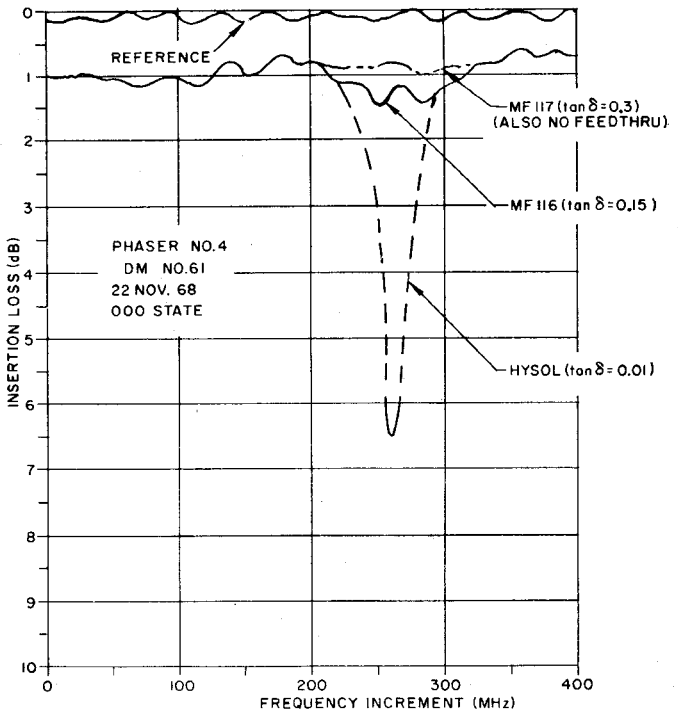

Fig. 7. VSWR versus isolation.

A second group of 15 phasers was fabricated using techniques identical to those used on the initial group of 10 except with improved feedthroughs. The feedthrough material had a dielectric loss tangent of 0.08 and a magnetic loss tangent of about 0.12, making the effective loss tangent about 0.15. Only 3 out of 15 elements exhibited resonances and the average peak absorption in those elements with resonances was 0.5 dB. These results are generally consistent with what would have been predicted from Fig. 5.

In order to compare the resonance reduction capability of several different feedthrough materials, a third experiment was conducted. A swept frequency loss measurement was made on a single phaser, using no feedthroughs and each of three different types of lossy feedthrough. The results from four sets of these measurements are shown in Table I. As an example, the measured insertion loss versus frequency for Phaser 4 is plotted in Fig. 7.

In conclusion, the absorption resonances and RF leakage which have long been associated with digital latching phasers can now be eliminated by a systematic choice of feedthrough material and dimensions. In addition, the feedthrough allows wider ferrite and waveguide assembly tolerances and results in a less expensive device.

TABLE I

LOSSY FEEDTHROUGH COMPARISON
PEAK ABSORPTION-RESONANCE AMPLITUDE (dB)

Type	Tan δ	Phaser 1	Phaser 2	Phaser 3	Phaser 4
1	0.01	8.0	2.8	2.3	5.5
2	0.15	1.5	0.2	0.2	0.6
3	0.3	1.0	0.2	0.2	0.3
None		0.2	0.2	0.2	0.2

REFERENCES

[1] D. H. Temme *et al.*, "A low cost latching ferrite phaser fabrication technique," presented at the 1969 G-MTT Int. Microwave Symp., Dallas, Tex.
[2] N. Marcuvitz, Ed., *Waveguide Handbook* (Radiation Lab. Series 10). Boston, Mass.: Boston Technical Publishers, 1967, pp. 32, 33.
[3] J. Frank, J. Kuck, and C. Shipley, "Latching ferrite phaser shifter for phased arrays," *Microwave J.*, Mar. 1967.

A Dominant Mode Analysis of Microstrip

R. P. WHARTON AND G. P. RODRIGUE

***Abstract*—A computer-aided numerical analysis of the dominant mode propagating in microstrip transmission line is reported, and the theoretical results are corroborated by experimental measurements. A region of almost complete circular polarization is found to exist at the surface of the dielectric, although most of the energy is concentrated directly beneath the strip conductor where the fields possess almost complete linear polarization.**

INTRODUCTION

This analysis of the field distributions in microstrip transmission lines has been carried out in two parts: a theoretical analysis yielding a numerical solution and an experimental study using a small YIG sphere as a field probe. The work was prompted by the knowledge that in order to satisfy all the boundary conditions, the microstrip mode has to be a combination of TE and TM modes existing simultaneously, thus forming a TE–TM hybrid mode. Yet, propagation constant data calculated under a TEM assumption yields good agreement with experimental results. In addition, a laboratory investigation has indicated the existence of a region of circular polarization as evidenced by the realization of a strongly nonreciprocal microstrip resonance isolator [1].

THEORETICAL ANALYSIS AND RESULTS

The theoretical approach [2] used here has been to solve the vector Helmholtz equations numerically for the longitudinal electric and magnetic fields. Since microstrip by its very nature is an open structure, a quantized model would require a subdivision of the region around it into an infinite number of mesh points. Thus it was necessary to enclose the region around the microstrip with a bounding wall. Experimentally, the microstrip fields are found to decay to zero far away from the center strip, thus in this work the longitudinal electric and magnetic fields were required to vanish at those walls. In the microstrip model the dielectric substrate is assumed to be linear, homogeneous, and isotropic. The lossless case is assumed so that the propagating mode is considered to have a z dependence of the form $e^{j(\omega t-\beta z)}$. The strip and ground plane are treated as being infinitely thin and perfectly conducting.

Finite-difference equation representations of the Helmholtz equations were derived for both longitudinal field components. The

Manuscript received August 19, 1971; revised November 5, 1971.
R. P. Wharton is with Schlumberger Well Services, Houston, Tex. 77001.
G. P. Rodrigue is with the School of Electrical Engineering, Georgia Institute of Technology, Atlanta, Ga. 30319.